Theoretical and Spectroscopic Study of Nickel(II) Porphyrin Derivatives

Cristhian Berríos,[†,‡] Gloria I. Cárdenas-Jirón,[*,‡] José F. Marco,[§] Claudio Gutiérrez,[§] and Maria Soledad Ureta-Zañartu[*,†]

Laboratorio de Electrocatálisis and Laboratorio de Química Teórica, Facultad de Química y Biología, Universidad de Santiago de Chile (USACH), Casilla 40, Correo 33, Santiago, Chile, and Instituto de Química Física "Rocasolano", CSIC, C. Serrano 119, 28006-Madrid, Spain

Received: August 21, 2006; In Final Form: January 11, 2007

A set of substituted (sulfonate, amino) nickel porphyrin derivatives such as phthalocyanine and phenylporphyrin was studied by spectroscopic (UV−vis, FTIR, XPS) and quantum-chemical methods. The Q and Soret bands were identified in the UV−vis spectra of aquo solutions of the tetrasulfo-substituted complexes and in DMF and ACN solutions of the amino-substituted phenylporphyrin and phthalocyanine Ni(II) complexes, respectively. In all the complexes the frontier molecular orbitals predict that the oxidation and reduction sites are localized on the ligand rather than in the metal atom. A natural bonding orbital (NBO) analysis of all the complexes showed that a two-center bond NBO between the pyrrolic nitrogens (N_{pyrr}) and the nickel atom does not exist, the $N_{pyrr}\cdots Ni$ interaction occurring instead by a delocalization from one lone pair of each N_{pyrr} toward one lone pair of the nickel atom, as estimated by second-order perturbation theory. The calculated values of electronic transitions between the frontier molecular orbitals are in good agreeement with the UV−vis data. At the theoretical level, we found that while the ligand effect is more important in the Q-band (∼16 kcal/mol), the substituent effect is more significant in the Soret band (∼9 kcal/mol). A good agreement was also found between the experimental and calculated infrared spectra, which allowed the assignment of many experimental bands. The XPS results indicate that the Ni(II) present in the phenylporphyrin structure is not affected by a change of the substituent (sulfonate or amino).

1. Introduction

Nickel phthalocyanines and porphyrins are interesting modifiers able to electropolymerize at diverse electrodes surfaces,[1,2] conferring them catalytic activity for many types of reactions, including oxygen reduction[3] and oxidation of compounds as chlorophenols,[1,2] methanol,[4,5] and other organics as alcohols and aldehydes,[6] hydrazine,[7,8] hydroxylamine,[9] etc. The catalytic activity depends on many factors and especially on the electronic structures, which are not fully understood, even though they have been investigated both with experiment and with quantum-chemical calculations at the density functional theory level (DFT) (B3LYP/6-31G(d)) by Zhang et al.[10] The complexes have also been used to model the vibrational spectra of some metallotetrasulfophthalocyanines[11] and to study the electronic structure, bonding, and properties of "unligated and ligated manganese tetraphenylporphyrine" using DFT methods.[12] It is most important to obtain spectroscopic data related with the structure of the metal macrocycles that can be correlated with the theoretical quantum-chemical results. In this sense X-ray photoelectron (XPS), Fourier-transform infrared (FTIR), and UV−vis spectroscopies are powerful tools to characterize the electronic structure of metallophthalocyanines and metalloporphyrins. XPS allows one to know the core-level spectra that give information on the chemical environments of the different atoms in the molecule.[13] The core electron binding energies of the central nitrogen atoms in a porphyrin are strongly affected by perturbations of the macrocycle, making N 1s XPS a sensitive probe of changes in charge distribution.[14,15] Due to the high molar absorption coefficient of these molecules in the UV−vis region, there is considerable interest in the characterization of the electronic structure of phthalocyanines and phenylporphyrins of nickel (NiPc and NiPP) molecules.

During the last years we have studied, using quantum-chemistry methods, several tetraazamacrocycles containing a transition metal atom. Reactivity indexes derived under the theoretical formalism of the density functional theory have been used to predict global and local reactivities of complexes participating in oxidation−reduction processes.[16−29] Charge-transfer mechanisms were proposed for several oxidation processes involving small substrates such as mercaptothiol, hydrazine, and carbon dioxide and classified in terms of the concepts of *through bond* or *through space*.[30−35]

The aim of this work is to study at the molecular level, using quantum chemistry, the ligand and substituent effects of a set of substituted Ni(II) macrocycles (NiPc and NiPP) to understand their experimentally observed spectroscopic behavior and to predict their eventual reactivities.

2. Experimental and Computational Aspects

2.1. Spectroscopic Characterization. Two water-soluble Ni(II) complexes were used: nickel tetrasulfophthalocyanine (NiTSPc); nickel tetrasulfophenylporphyrin (NiTSPP). Two water-insoluble Ni(II) compounds were used: nickel tetraaminophthalocyanine (NiTAPc); nickel tetraaminophenylporphyrin (NiTAPP). The molecular structures of the studied nickel complexes are given in Figure 1.

* Authors to whom correspondence should be addressed. E-mail: mureta@lauca.usach.cl (M.S.U-Z.); gcardena@lauca.usach.cl (G.I.C.-J.).
† Laboratorio de Electrocatálisis, Universidad de Santiago de Chile.
‡ Laboratorio de Química Teórica, Universidad de Santiago de Chile.
§ Instituto de Química Física "Rocasolano", CSIC.

10.1021/jp0653961 CCC: $37.00
Published on Web 03/17/2007

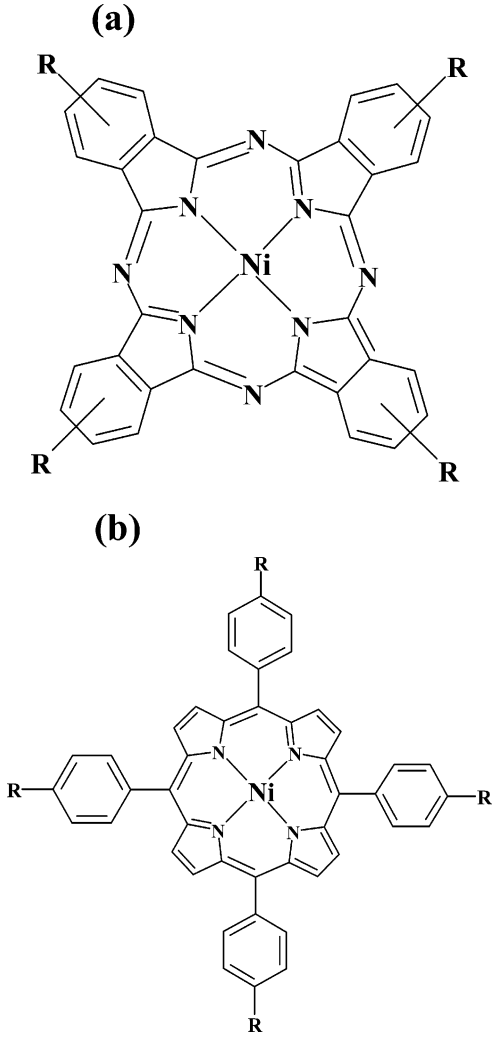

Figure 1. General view of the molecular structure of nickel complexes: (a) nickel tetrasubstituted phthalocyanine NiTRPc; (b) nickel tetrasubstituted phenylporphyrin NiTRPP (R= sulfonate, amino).

Ni^{II}TSPc (Aldrich), Ni^{II}TSPP, Ni^{II}TAPc, and Ni^{II}TAPP (MID-Century, Posen, IL) and all other chemicals (Merck, pa) were used as received. The solutions of NiTSPc and NiTSPP were prepared in water (deionized and twice distilled), NiTAPc was prepared in ACN, and NiTAPP was prepared in DMF.

A Varian UV−vis spectrophotometer, model Cary 1E, provided with a double-array detector and a Bruker IFS 66v FTIR spectrometer were used. XPS data were recorded with a triple channeltron CLAM2 analyzer, under an operating vacuum in the range 10^{-9} Torr, using Mg Kα radiation and a constant analyzer transmission energy of 20 eV. The powdered samples were supported on double-sided adhesive conductive carbon tape. All the spectra were recorded at takeoff angles of 90°. All binding energy values were referenced to the main C 1s signal of the porphyrin which is located at 284.8 eV. All the spectra were computer-fitted. Spectral areas were calculated by peak integration after Shirley background subtraction.[36] Relative atomic concentrations were calculated using tabulated atomic sensitivity factors.[37]

2.2. Computational Aspects. Theoretical calculations using quantum chemistry for the NiTSPc, NiTAPc, NiTSPP, and NiTAPP complexes in the gas phase were performed. Optimized molecular structures were calculated with the B3LYP exchange correlation functional that contains a Becke's three-parameter hybrid exchange functional, the exact Hartree Fock, Slater, and Becke exchanges, and also contains the LYP correlation functional, a Vosko, Wilk, and Nusair (VWN) local functional, and a Lee, Yang, and Parr (LYP) nonlocal functional.[38] All the calculations were performed with the Jaguar package.[39] The basis set used was an effective core potential (ECP) named as LACVP for the nickel atom and a 6-31G basis set for the lighter atoms such as carbon, nitrogen, oxygen, sulfur, and hydrogen, including for all the atoms a set of five d polarization functions. Furthermore, a set of s and p diffuse functions (LACVP(d)++) was also included. Since the NiTSPc and NiTSPP complexes present four SO_3^- groups which have a total charge of −4, it was necessary to include diffuse functions in the respective calculations. The inclusion of diffuse functions is especially recommended in anionic systems, because it allows a better relaxation of the electronic density localizing part in the additional atomic orbitals (s,p), so decreasing the electronic repulsion. The amino complexes (NiTAPc, NiTAPP) were calculated in their neutral states. The numbers of basis functions of the complexes were 1082 and 874 basis functions for the NiTSPc and NiTAPc complexes, respectively, and 1262 and 1054 basis functions for the NiTSPP and NiTAPP complexes, respectively. As can be seen, for the same substituent the number of basis functions is larger for the PP ligand, and hence these are larger than for the complexes with the Pc ligand. All the systems studied contain a Ni(II) atom and are closed-shell systems; therefore, the multiplicity used in all the calculations was that of a singlet. A natural bond orbital (NBO) analysis was performed for each complex to understand the electronic structure of the ligand and of the nickel atom in terms of a Lewis-like structure and also to know the possible delocalizations that occur in the complexes. This analysis was done with the NBO 5.0[40] software included in the Jaguar package. IR spectra were also obtained in the gas phase at the B3LYP/LACVP(d)++ level and compared to the experimental data. The theoretical rationalization of the UV−vis experimental spectra was done using the delta method, that is obtaining the energy difference between the molecular orbitals calculated with B3LYP/LACVP(d)++. Unfortunately, because of the large size of the complexes studied here, we were not able to obtain the theoretical UV−vis spectra by a more precise technique like the time-dependent density functional method.

3. Results and Discussion

3.1. X-ray Photoelectron Spectroscopy (XPS). To obtain experimental evidence about the influence of the substituents in the physical structure of the Ni macrocycles, XP spectra from the PP powdered complexes were recorded. The N 1s spectrum recorded from NiTSPP is shown in Figure 2A. The spectrum shows a main peak (77% of the total spectral area) at 398.8 eV, which is characteristic of the pyrrolic nitrogen in the NiTSPP structure,[41] and some other minor peaks at 399.9 eV (11%) and 401.5 eV (12%), the origin of the latter being uncertain. The component located at 399.9 eV might be due to a protonated nitrogen species[42] arising from some small degree of demetalization, perhaps due to X-ray-induced sample degradation.[43] It might also arise from some small free-base porphyrin impurity in the original sample, since that binding energy is characteristic of the central protonated nitrogen present in the structure of free-base porphyrins.[44] Finally we would comment that high binding energy nitrogen species (in the range 401.5−403.0 eV) are usually observed in the N 1s XP spectra of porphyrins[42,45,46] and they have been associated with shakeup satellites.[47]

The Ni 2p spectrum recorded from the NiTSPP monomer consists of a relatively narrow spin−orbit doublet (Figure 2B) characterized by binding energies of the Ni $2p_{3/2}$ and Ni $2p_{1/2}$

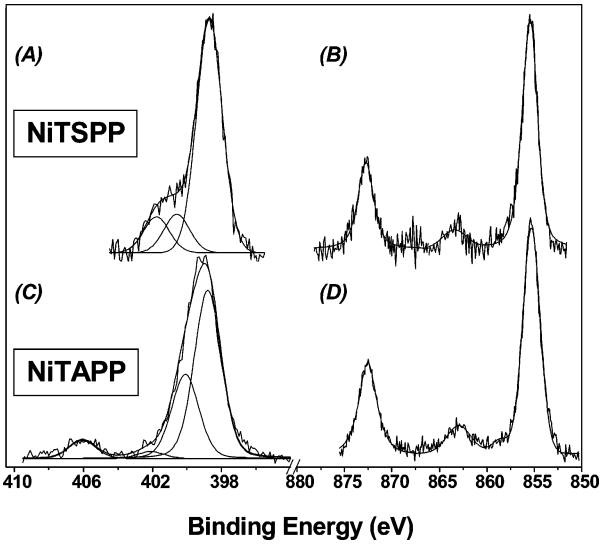

Figure 2. (A) N 1s and (B) Ni 2p spectra recorded from NiTSPP. (C) N 1 s and (D) Ni 2p spectra recorded from NiTAPP.

TABLE 1: Atomic Relations from the Analysis of the XPS Data

sample (powder)	Ni/C	N/C	O/C	S/C
NiTSPP	0.015	0.046	0.324	0.054
NiTAPP	0.014	0.103	0.175	

core levels of 855.4 and 873.0 eV, respectively. These values are similar to those reported for other Ni porphyrins.[41,44,48] The spectrum shows a weak satellite at 863.1 eV which has been also reported previously.[49] The absence of strong shakeup satellite structure confirms the diamagnetic nature of Ni(II) in the structure of TSPP. In fact, it is known that the NiTSPP metalloporphyrin is diamagnetic.[44]

The N 1s spectrum recorded from the NiTAPP powder sample is shown in Figure 2C. It contains several contributions. The main one at 398.8 eV (60%) is associated with the pyrrolic nitrogen bonded to the Ni(II) in the porphyrin structure, while the contribution at 400.0−400.2 eV (30%) is associated with the presence of the $-NH_2$ groups. Some other minor components are observed at higher binding energies, 402.1 eV (3%, shakeup satellites) and 405.7 eV (7%, inelastic scattering[47]).

The Ni 2p spectrum of NiTAPP is very similar to that of NiTSPP (Figure 2D). The binding energies of the main Ni $2p_{3/2}$ and Ni $2p_{1/2}$ core levels are 855.4 and 873.0 eV, respectively. The spectrum also shows a very weak satellite at 863.1 eV. Similarly to the NiTSPP case, the weakness of this satellite indicates that the Ni(II) present in the NiTAPP is mainly diamagnetic in nature.

The S 2p spectrum of NiTSPP was also recorded (not shown). It consisted of a doublet with the energy of the main $2p_{3/2}$ line located al 168.1 eV, which we associate with the SO_3^- groups.

Finally, and as expected, the C 1s spectra recorded from both NiTSPP and NiTAPP show the three components, at 284.8 eV (carbons pertaining to the phenyl rings), at 286.3 eV (pyrrole C atoms), and at 288.5 eV (pyrrole carbon shakeup transitions), characteristic of porphyrins.[47,50]

The atomic ratios calculated from the XPS spectra are shown in Table 1. The data indicate that the Ni load is very similar in both samples. The N/C atomic ratio is higher in NiTAPP than in NiTSPP, due to the presence of amino groups in the first compound. Obviously, only NiTSPP shows the presence of the S from the SO_3^- groups.

The results indicate that the nature and characteristic binding energies of the Ni 2p core levels of the Ni(II) present in these compounds are unaffected by the changes in the substituents. Besides, there is no evidence that these changes affect the binding energy of the N 1s core level of the four pyrrolic nitrogens.

3.2. Molecular Structure. The results of the optimized molecular structures at the DFT level of calculation for the NiTSPc, NiTAPc, NiTSPP, and NiTAPP complexes are shown in Figure 3. In general terms, a ligand effect of the phthalocyanine (Pc) with respect to the phenylporphyrin (PP) is observed. A comparison of ligands for a given substituent shows that the complexes with PP ligand present an important distortion of the porphyrin, with respect to those complexes with the Pc ligand, which are nearly planar structures (Figure 3a,b) with C_1 point group. The distortion is produced in the pyrrolic rings and is about 10° with respect to the planar central region of the porphyrin.

For the PP ligand, the optimized structures predict for both NiTSPP and NiTAPP that the phenyl groups are localized perpendicularly to the porphyrin ligand, suggesting that this spatial conformation minimizes the electronic repulsion between the hydrogen atoms in β positions at the porphyrin ligand and those hydrogens belonging to the phenyl group. For both complexes, NiTSPP and NiTAPP, the optimized structure predicts that the phenyl groups are localized at 120° with respect to the porphyrin ligand.

The comparison of the calculated bond lengths for all the complexes showed that only the Ni−N bonds (r_{Ni-N}) present an important change between them, the remaining bond lengths being very similar in all the complexes. The results indicated that in each complex the four Ni−N bonds have the same length, approximately 1.9 Å in agreement with both experimental[51] and calculated data.[11,52] We also found that no substituent effect exists for the Pc ligand; the value of r_{Ni-N} calculated for both NiTSPc and NiTAPc is 1.93 Å. In the case of the PP ligand, the calculated values of r_{Ni-N} were 1.98 Å for NiTSPP and 1.96 Å for NiTAPP. Thus, the complexes with the PP ligand have a Ni−N bond distance that is slightly larger than that for those containing the Pc ligand. These results could suggest that in the complexes with the Pc ligand there would be a higher electronic density in the Ni−N bond. In section 3.3.2 we will discuss the NBO analysis of these molecules, which confirms this suggestion.

3.3. Condensed to Atoms Properties. *3.3.1. Molecular Orbital Description.* Frontier molecular orbitals (MO), HOMO (highest occupied MO), and LUMO (lowest unoccupied MO) of the NiTAPc, NiTSPc, NiTAPP, and NiTSPP complexes were obtained at the B3LYP/LACVP(d)++ level of calculation. Frontier MOs are very useful in a theoretical calculation because they provide information about the molecular reactivity, which usually occurs in the frontier of a system. The local regions where the frontier MOs are localized represent the most probable reactive sites, that is, sites that have a major probability to be present in an oxidation or reduction process. In general, we found that in all the studied systems the frontier MOs HOMO and LUMO are localized on the ligand rather than on the nickel atom, meaning that in all the complexes studied an oxidation or reduction process would be carried out on the ligand. We also investigated if some molecular orbital near the frontier of the system has any contribution of the metal atom. In the case of occupied MOs, we found for the sulfonated complexes (NiTSPP, NiTSPc) a nickel contribution in HOMO-9 and HOMO-10 and for the amino complexes (NiTAPP, NiTAPc) a nickel contribution was predicted from HOMO-5 to HOMO-8. The analysis of the virtual MOs led in the four complexes to

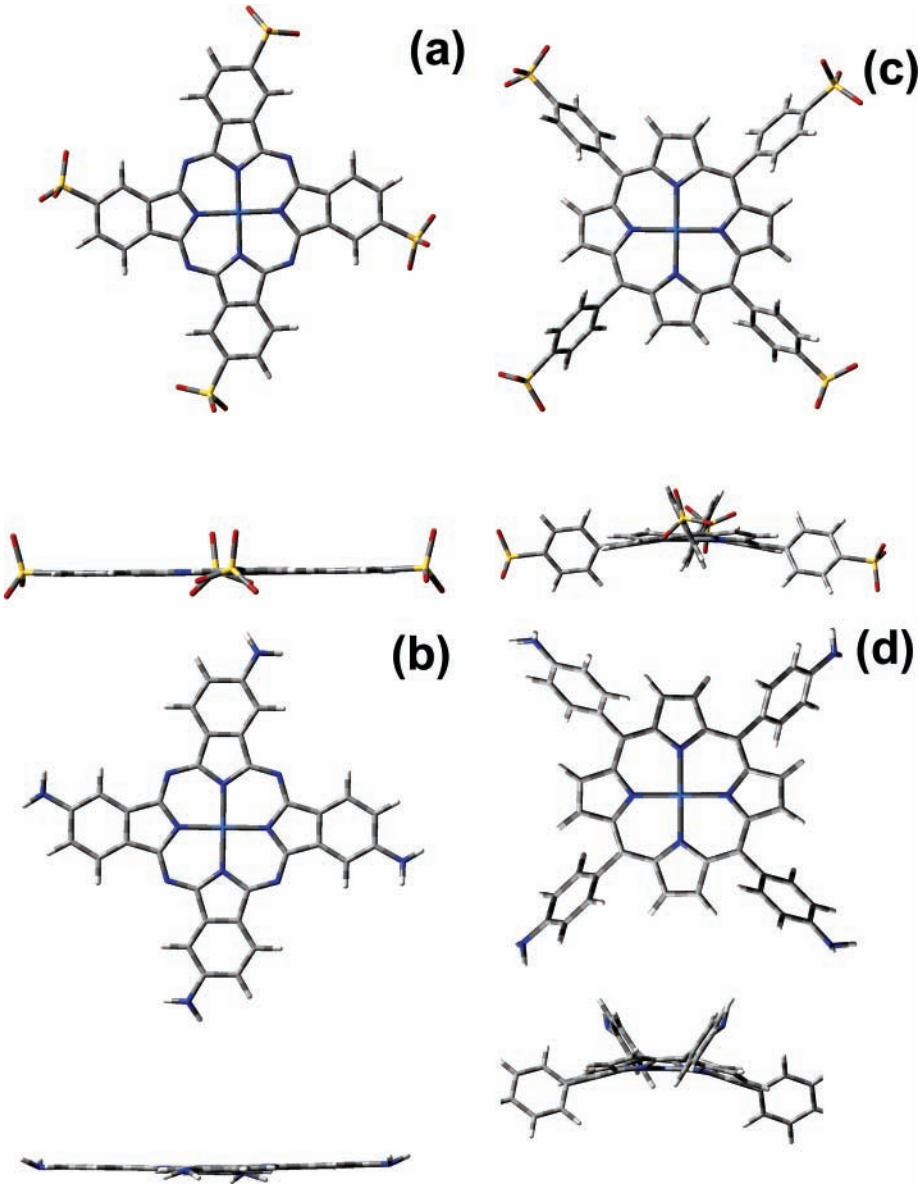

Figure 3. Fully optimized molecular structures at the B3LYP/LACVP(d)++) level of calculation in a front and side view: (a) NiTSPc; (b) NiTAPc; (c) NiTSPP; (d) NiTAPP.

only one MO, LUMO+2 with a strong contribution of nickel. These results would indicate that if the complexes studied here were chosen for an oxidation or reduction process where the charge transfer between the donor and the acceptor species occurs with a participation of the metal atom, then a reduction process would be more probable than an oxidation process.

We also found that the change of the substituent (NH_2, SO_3^-) does not produce a significant modification of the frontier molecular orbitals. In contrast, the calculations predict that the change of the ligand (Pc, PP) produces an important change in the frontier MOs. Although the frontier MOs are localized on the ligand rather than on the nickel atom, the position where they are localized in the complexes is different. As an illustration, we show in Figure 4 only the calculated frontier MOs (HOMO, LUMO) for the NiTSPc and NiTSPP complexes. It can be observed that in the Pc ligand the HOMO molecular orbital is localized only on the carbon atoms neighboring the pyrrolic nitrogens. In the PP ligand, the HOMO molecular orbital is preferently localized both on the four *meso* carbons and on the four pyrrolic nitrogens. In the case of the LUMO MO, for the Pc ligand it is localized both on the carbon atoms of two pyrrolic rings and on the four aza nitrogens and on two pyrrolic nitrogens. In the case of the PP ligand, the LUMO MO is localized on the *meso* carbon atoms, on two pyrrolic nitrogens localized in opposite places, and on the carbon atoms belonging to the pyrrole rings.

From an energetic point of view, we found that the energy gap between the frontier MOs ($\epsilon_{LUMO} - \epsilon_{HOMO}$) is very similar for the complexes containing the same ligand but a different substituent. In a DFT framework, this energy gap is associated with the molecular hardness ($\eta = (\epsilon_{LUMO} - \epsilon_{HOMO})/2$)[53] that gives account of the molecular reactivity. A higher η implies a lower reactivity and therefore a higher stability. In the case of the Pc ligand, the molecular hardness is 24.9 kcal/mol for NiTSPc and 24.2 kcal/mol for NiTAPc, showing that the substituent effect is very low (0.7 kcal/mol). For the PP ligand, the situation is similar: the absolute values of η are 32.9 kcal/mol in NiTSPP and 31.7 kcal/mol in NiTAPP, the substituent effect being only 1.2 kcal/mol. On the contrary, the ligand effect is more important than the substituent effect, the former having a value of 8.0 kcal/mol when NiTSPc is compared to NiTSPP and a value of 7.4 kcal/mol for the comparison between NiTAPc and NiTAPP. We also see that, in terms of the molecular

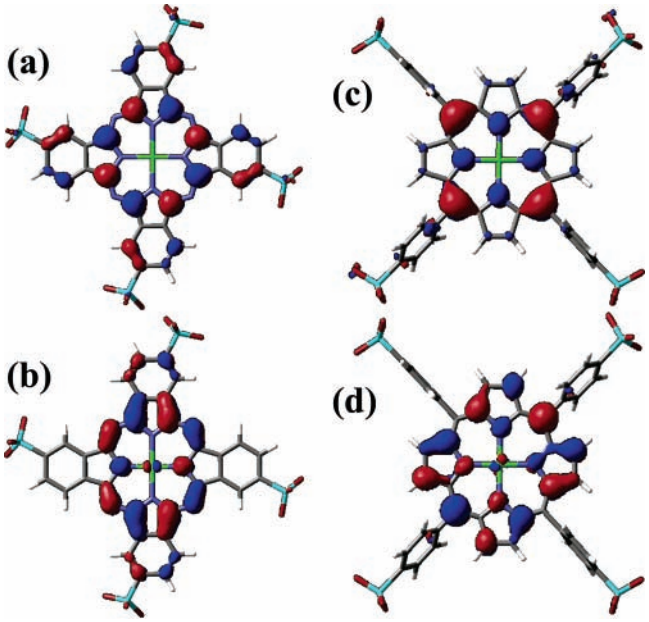

Figure 4. Surfaces of HOMO and LUMO frontier molecular orbitals obtained at the B3LYP/LACVP(d)++ level of theory: (a) NiTSPc/HOMO; (b) NiTSPc/LUMO; (c) NiTSPP/HOMO; (d) NiTSPP/LUMO.

reactivity, the molecules containing a PP ligand have a lower reactivity (higher η).

In summary, both from a qualitative point of view (composition of molecular orbitals) and from a quantitative point of view (energetics of MOs) there is no important substituent effect (NH_2, SO_3^-) but rather an important ligand effect (Pc, PP).

3.3.2. Natural Bond Orbital Analysis. The natural bond orbital (NBO) analysis was also used to analyze the substituent effect and the ligand effect on the nickel complexes. The NBO analysis provides information about the Lewis and the non-Lewis (Rydberg) structure. It corresponds to the hypothetical structure of Lewis. Therefore, the electrons are located in bonds (BD) (electron pairs centered on two atoms), lone pairs (LP) (electron pairs centered on one atom), and core pairs (CR) (electron pairs centered on the core of one atom). Each one of these is defined in this methodology as NBO. The calculations of NBOs predict that the complexes studied do not present a BD between the N-pyrrolic (N_{pyrr}) and the nickel atom (Ni); that is, there is not an electron pair centered between N_{pyrr} and Ni. In contrast, in all the complexes the interaction between these atoms is seen through an electronic delocalization between bond orbitals from LP(1) N_{pyrr} to LP(5) Ni. All NBOs named as LP(1) N_{pyrr} present a 33% s character and a 67% p character; that is, they are sp^2 hybrid orbitals. The NBO LP(5) of the nickel atom is a d pure orbital. The electronic delocalizations are estimated by second-order perturbation theory (Table 2) from the energy $E^{(2)}$ associated with the donor−acceptor interaction between two NBOs.[40] Some of the most important of these interactions occurring in the complexes, that is those presenting a stronger delocalization with the higher value of $E^{(2)}$, are reported in Table 2. Although all the complexes present a strong delocalization LP(1) N_{pyrr} → LP(5) Ni, the complexes containing the Pc ligand (NiTSPc, NiTAPc) show a larger delocalization by about 7 kcal/mol than the complexes with a PP ligand. This would suggest that the electronic population on the nickel atom is slightly higher in the Pc ligand than in the PP ligand. In fact, this has a value for NiTAPc of 27.058 and for NiTSPc of 27.065. In NiTSPP the electronic population on the nickel atom is 27.023, and in NiTAPP is 27.040. These results are consistent with the optimized bond lengths for the Ni−N bond discussed in section 3.2, which were 1.92 Å for the Pc ligand and 1.96−1.98 Å for the PP ligand. A shorter bond length favors a higher electronic delocalization. Again, there is no substituent effect but rather an effect of the ligand change. Another kind of delocalization predicted by second-order perturbation theory was LP(1) N_{pyrr} → LP*(6) Ni, that is, between a bond orbital (LP(1) N_{pyrr}) and one antibond orbital (LP*(6) Ni). The latter NBO has a 100% s character. Again, the complexes with Pc ligand present a higher delocalization of about 9 kcal/mol with respect to the complexes with PP ligand (see Table 2). The NBO analysis also shows that a strong interaction like LP(1) Ni → RY*(1) N_{pyrr} occurs, where RY* is referred as the Rydberg shell that is beyond of the valence shell. The results of $E^{(2)}$ obtained for the four pyrrolic nitrogens in each complex give values of 68−81 kcal/mol for those containing the Pc ligand and values of 41−65 kcal/mol for the complexes with PP ligand. This again shows that a ligand effect is more important than a substituent effect.

In general, the natural population analysis shows similar results for the common atoms in the four complexes, with the exception of some atoms. For example, the comparison of NiTAPc with NiTSPc shows that both complexes have a charge of −0.60 for the pyrrolic nitrogens and of −0.48 for the aza nitrogens. The nickel atom has a value of 0.94 for both complexes, and the C-α with respect to N_{pyrr} has a value of about 0.41. Some differences are observed in the C-β with respect to N_{pyrr} which are sligthly more negative in NiTAPc

TABLE 2: Second-Order Perturbation Energy $E^{(2)}$ (Donor → Acceptor) (kcal/mol) Calculated at the B3LYP/6-31G(d)++ Level of Calculation for the Donor−Acceptor Interactions with the Higher Energy

donor	acceptor	$E^{(2)}$
	NiTSPc	
LP(1) N^1_{pyrr}[a]	LP(5) Ni	41.43
LP(1) N^1_{pyrr}	LP*(6) Ni	67.48
LP(1) N^2_{pyrrr}	LP(5) Ni	41.06
LP(1) N^2_{pyrr}	LP*(6) Ni	67.33
LP(1) N^3_{pyrr}	LP(5) Ni	40.98
LP(1) N^3_{pyrr}	LP*(6) Ni	66.77
LP(1) N^4_{pyrr}	LP(5) Ni	41.45
LP(1) N^4_{pyrr}	LP*(6) Ni	67.31
	NiTAPc	
LP(1) N^1_{pyrr}	LP(5) Ni	41.83
LP(1) N^1_{pyrr}	LP*(6) Ni	67.83
LP(1) N^2_{pyrr}	LP(5) Ni	41.53
LP(1) N^2_{pyrr}	LP*(6) Ni	66.68
LP(1) N^3_{pyrr}	LP(5) Ni	41.61
LP(1) N^3_{pyrr}	LP*(6) Ni	67.11
LP(1) N^4_{pyrr}	LP(5) Ni	41.88
LP(1) N^4_{pyrr}	LP*(6) Ni	67.54
	NiTSPP	
LP(1) N^1_{pyrr}	LP(5) Ni	34.54
LP(1) N^1_{pyrr}	LP*(6) Ni	58.15
LP(1) N^2_{pyrr}	LP(5) Ni	34.74
LP(1) N^2_{pyrr}	LP*(6) Ni	58.32
LP(1) N^3_{pyrr}	LP(5) Ni	34.58
LP(1) N^3_{pyrr}	LP*(6) Ni	57.67
LP(1) N^4_{pyrr}	LP(5) Ni	34.86
LP(1) N^4_{pyrr}	LP*(6) Ni	58.34
	NiTAPP	
LP(1) N^1_{pyrr}	LP(5) Ni	36.86
LP(1) N^1_{pyrr}	LP*(6) Ni	60.97
LP(1) N^2_{pyrr}	LP(5) Ni	37.40
LP(1) N^2_{pyrr}	LP*(6) Ni	61.41
LP(1) N^3_{pyrr}	LP(5) Ni	37.14
LP(1) N^3_{pyrr}	LP*(6) Ni	61.59
LP(1) N^4_{pyrr}	LP(5) Ni	37.52
LP(1) N^4_{pyrr}	LP*(6) Ni	61.36

[a] Superscripts 1−4 refer to each pyrrolic nitrogen.

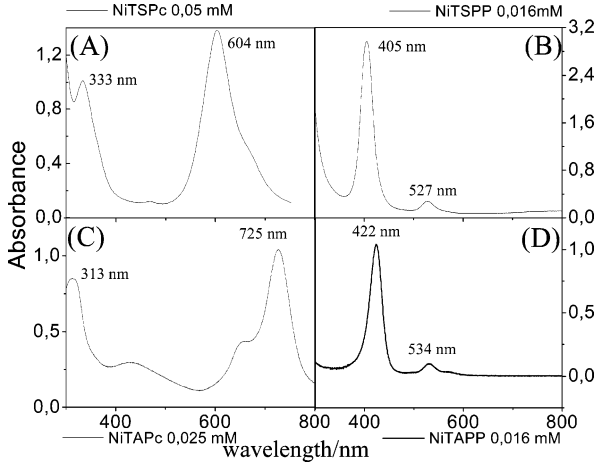

Figure 5. UV−vis spectra in solution: (A) 0.05 mM NiTSPc/buffer at pH 11; (B) 0.016 mM NiTSPP/buffer at pH 11; (C) 0.025 mM NiTAPc/ACN−PTBA; (D) 0.016 mM NiTAPP/DMF−PTBA.

(−0.06, −0.12) than in NiTSPc (−0.01, −0.11). The charge on the carbon atom bonded to the substituent is completely different, as expected, due to the ability of the substituent to be electron withdrawing or an electron donor. In NiTAPc this carbon atom has a charge of 0.16, confirming the electron donor character of the amino group. However, in NiTSPc this carbon atom presents a charge of about −0.30, showing the electron-withdrawing character of the sulfonate group. For the pair of complexes with PP ligand, NiTSPP and NiTAPP, a very similar behavior is obtained. However, when we compare the charges for complexes containing the same substituent but different ligands, we found several differences which should be mentioned. For example, in NiTSPc the nickel atom has a charge of 0.94 and in NiTSPP it has a charge of 0.98. Why does the metal atom lose more electrons in NiTSPP although it has a longer N−Ni bond length than in NiTSPc? The answer could be in the NBO analysis. From this, we found that in NiTSPP there is a very strong interaction from LP(1) Ni, that is a d pure orbital, to RY*(8) C-α (C-α, that is neighboring to one pyrrolic nitrogen) which is nearly a p orbital (87%). This occurs only in one C-α. The $E^{(2)}$ value for this interaction is 247.3 kcal/mol, a higher value than the results shown in Table 2. This value would indicate that an electronic delocalization occurs and explains why the nickel atom loses more electrons in NiTSPP than in NiTSPc. For the NiTAPc/NiTAPP pair the situation is very similar; the nickel charge is 0.94 for NiTAPc and 0.96 for NiTAPP. For the latter, we found from the NBO analysis several interactions from LP(1) Ni to RY*(5), RY*(8), and RY*(9) of one C-α bonded to one pyrrolic nitrogen, which is bonded directly to the nickel atom. The energies associated with this kind of interaction are in the range 14.4−17.4 kcal/mol. These results indicate that electronic density is transferred from the nickel atom to the ligand although it is of lower energy than in NiTSPP. Furthermore, we found in all of the four complexes that an interaction from LP(1) Ni to some RY* of the pyrrolic nitrogens occurs.

3.4. UV−Vis Spectroscopy. The UV−vis spectra of the complexes in solution were recorded for Ni(II) complexes in the range 300−800 nm using pure water as solvent for NiTSPc and NiTSPP, DMF for NiTAPP, and ACN for NiTAPc (Figure 5). The characteristic Soret and Q bands appear at different wavelengths (see Table 3), in agreement with the different structure of these compounds. It is known that changes in the solvent do not dramatically change the UV−vis absorption spectra of these organometallic compounds[54] (the use of different solvents was necessary due to the water insolubility of amino complexes). Substituted nickel porphyrin complexes show a Soret band (near 400 nm) more intense than that of the respective phthalocyanines (near 310 nm), whereas the Q-band near 530 nm had a very low absorbance. Phthalocyanines show an intense Q-band near 600 nm which is shifted to near 700 nm when the amino replaces the sulfonated groups.

TABLE 3: Experimental Energies (eV) of the Bands in the UV−Vis Spectra of the Different Nickel Complexes in Solution and Calculated Values (eV) of Electronic Transitions in the Gas Phase at the B3LYP/LACVP(d)++ Level of Calculation[a]

	expt		calcd	
nickel complex (solvent)	Soret band	Q band	Soret band	Q band
NiTSPc (water)	3.72	2.05	2.82 (3.64)	2.16 (2.17)
NiTAPc (ACN)	3.96	1.71	3.20 (3.04)	2.10 (2.03)
NiTSPP (water)	3.06	2.35	3.04 (3.03)	2.85 (2.92)
NiTAPP (DMF)	2.94	2.32	3.04 (3.06)	2.75 (2.68)

[a] The energies calculated for the complexes in the solution phase are given in parentheses.

From the theoretical point of view, a UV−vis spectrum can be understood in terms of an electronic transition between the frontier molecular orbitals (HOMO, LUMO) and also between occupied and unoccupied molecular orbitals near the frontier of the system, a situation that also applies to the MPc complexes.[55] In particular, Gouterman was the first to propose in the 1960s the four-orbital model to explain the absorption spectra of porphyrins.[56,57] According to this model, the absorption bands in porphyrin systems arise from transitions between two HOMOs (HOMO and HOMO-1) and two LUMOs (LUMO and LUMO+1), the nature of the metal center and of the substituents on the ring affecting the relative energies of these transitions.

Using quantum chemistry, we calculated with B3LYP/LACVP(d)++ the molecular orbitals, and then using the delta method, we determined the possible electronic transitions associated with both the Soret and Q-bands and compared them with the observed experimental bands. In general, a good agreement is found between the calculated and observed bands, as can be seen in Table 3. The calculations predict for the complexes with PP ligand differences with respect to the experimental value of 0.02 eV (0.7%) (NiTSPP) and 0.1 eV (3.4%) (NiTAPP) for the Soret band and of 0.50 eV (21%) (NiTSPP) and 0.43 eV (19%) (NiTAPP) for the Q-band. For the complexes containing a Pc ligand, we obtained for the Soret band differences of 0.90 eV (24%) (NiTSPc) and 0.76 eV (19%) (NiTAPc). In the case of the Q-band, the deviations from the experimental values are of about 0.11 eV (5%) (NiTSPc) and 0.39 eV (23%) (NiTAPc). In general, the complexes with the PP ligand show a better agreement between the theoretical and experimental results for the Soret band than the complexes with the Pc ligand. However, with the exception of NiTSPc, the predicted Q-bands present deviations of about 20% with respect to the experimental values.

On the other hand, from the calculations obtained with B3LYP/LACVP(d)++ we found for the four complexes studied that the unoccupied molecular orbitals LUMO and LUMO+1 are degenerate; that is, they have the same energy. However, the sets of HOMO and HOMO-1 do not present the same behavior: these molecular orbitals are not degenerate and present an energy difference which is higher for the complexes with the Pc ligand whose values are 0.7 eV for NiTSPc and 1.1 eV for NiTAPc. In the case of the complexes with the PP

TABLE 4: Experimental and Calculated Scaled Vibrational Frequencies (cm^{-1}) and Their Respective Assignments of Vibration Normal Modes for the Substituted Nickel Complexes[a]

	NiTSPc (a)		NiTAPc (b)	
assgnt	expt	calcd	expt	calcd
(b) stret N−H amino			3328	3429, 3430, 3516
stret C−H Ar	3436	3083, 3086, 3087, 3088, 3089, 3094, 3099	3205	3074, 3083, 3087, 3090
stret C−C Ar	1635	1543, 1570, 1582	1610	1578, 1588
C−N pyrrol				
C−H Ar out of plane				
C−N aza				
(a) stret S−O sulfonate asymm	1189	1172, 1174, 1177		
(a) stret S−O sulfonate symm	937, 970, 1033	922, 956	985	969
(b) bend N−H amino				

	NiTSPP (c)		NiTAPP (d)	
assgnt	expt	calcd	expt	calcd
(d) stret N−H amino			3440	3353, 3406, 3453, 3513, 3523, 3532, 3574, 3641
stret C−H Ar pyrrol	3436	3076, 3083, 3089, 3117, 3120, 3124, 3138	3118, 3210, 3363, 3453	3072, 3079, 3089, 3118, 3120, 3125, 3130
stret C−C pyrrol	1635	1591, 1597, 1606, 1625		1592, 1597, 1604, 1613, 1628, 1640
C−C Ar				
C−H Ar out of plane				
pyrrol out of plane (c) stret S−O sulfonate asymm	1184	1166, 1176, 1180	1172	1139
(d) bend N−H amino				
stret C−C Ar pyrrol out of plane	1125	1081, 1095		1067, 1072, 1078, 1091, 1106, 1118, 1122
(d) bend N−H amino				
(c) stret S−O sulfonate symm	1040	933, 942		

[a] Calculated values were obtained at the B3LYP/LACVP*++ level of calculation. Key: stret, stretching; bend, bending.

ligand, the energy difference between HOMO-1 and HOMO is of 0.2 eV for NiTSPP and of 0.3 eV for NiTAPP. This molecular orbital picture would explain why the UV−vis spectra of the porphyrin derivatives present two main characteristic bands (Soret, Q) instead of a single band, as would be expected if HOMO-1 and HOMO are degenerate. In this work, we assigned at the theoretical level the Soret band for the complexes with Pc and PP ligands to the transitions HOMO-1 (π) → LUMO (π^*) and HOMO-1 (π) → LUMO+1 (π^*), because both transitions present the same energy value. We assigned the Q-band to the transitions HOMO (π) → LUMO (π^*) and HOMO (π) → LUMO+1 (π^*). We also investigated how the ligand and the substituent effect are reflected in the UV−vis spectra. In relation to the predicted Q-band, we noted that the ligand effect (16 kcal/mol for the pair NiTSPc/NiTSPP and 15 kcal/mol for NiTAPc/NiTAPP) is more important than the substituent effect (1.4 kcal/mol, NiTSPc/NiTAPc, and 2.3 kcal/mol, NiTSPP/NiTAPP), as mentioned in section 3.3.1 in the analysis of the frontier molecular orbitals. This result could be explained because the MOs that participate in the Q-bands are localized on the macrocycle (ligand). An opposite behavior is found for the Soret band, the ligand effect having a value of 5.1 kcal/mol for the pair NiTSPc/NiTSPP and 3.7 kcal/mol for the pair NiTAPc/NiTAPP, while the substituent effect is, with the exception of NiTSPP/NiTAPP that does not present a change, 8.8 kcal/mol for NiTSPc/NiTAPc. So, while the ligand effect is more important in the Q-band, the substituent effect is more significant in the Soret band. For the latter, this result is understood in terms of the composition of HOMO-1 that presents an important contribution of the substituents $-NH_2$ and $-SO_3^-$ for NiTAPc and NiTSPc, respectively. With the aim to improve the values of the electronic transitions assigned to both the Soret and Q bands, we did single-point calculations in solution phase using the optimized geometry obtained in the gas phase (B3LYP/LACVP(d)++), and then we determined the respective electronic transitions using the delta method. The calculations in the solution phase were done with the Jaguar package[39] using a self-consistent reaction field (SCRF) determined by numerical solution of the Poisson−Boltzmann equations, representing the solvent as a layer of charges at the molecular surface, which serves as a dielectric continuum boundary. The solvents chosen were the same used in the experimental work: water for the sulfonated complexes (NiTSPc, NiTSPP); dimethylformamide for NiTAPc; acetonitrile for NiTAPP. The results showed that in general the trends of the electronic transitions are the same, with the exception of the Soret band of NiTSPc where the deviation with respect to experimental energy decreased from 24% (gas phase) to 2% (solution phase). This can be explained in terms of the MO involved in the Soret band, a transition HOMO-1 → LUMO and HOMO-1 → LUMO+1. HOMO-1 is localized on the substituent $-SO_3^-$ which is localized in the periphery of the complex, and the continuum model used in the calculation with solvent must affect mainly the substituent due to its nearness to the periphery and to the net charge of −1 for each group and of −4 for the whole complex. Both complexes with sulfonate groups present a very high solvation energy, −414.0 kcal/mol for NiTSPc and −397.7 kcal/mol for NiTSPP. On the contrary, in the complexes with the amino group the solvation energy is much lower, −36.3 kcal/mol for NiTAPc and −37.5 kcal/mol for NiTAPP.

3.5. Fourier Transform Infrared Spectra (FTIR). It is known that the vibrational spectrum of coordination compounds shows ligand vibrations in the high-frequency region (4000−600 cm^{-1}), whereas the metal−ligand vibrations appear in the low-frequency region (below 600 cm^{-1}).[58] The Pc skeleton from vibrations in the benzene ring in interaction with the pyrrolic ring appears between 700 and 400 cm^{-1}, a band attributed to

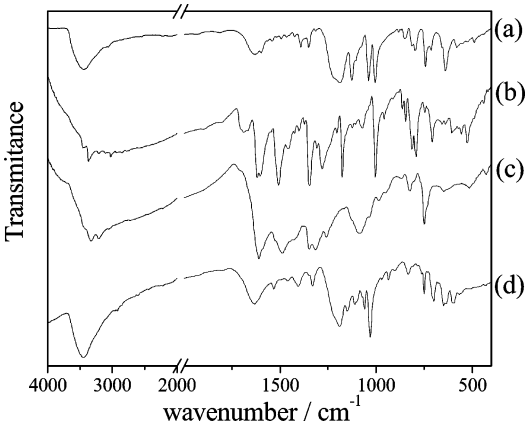

Figure 6. FTIR spectrum of (a) NiTSPP, (b) NiTAPP, (c) NiTAPc, and (d) NiTSPc in KBr pellets.

nonplanar deformation of C−H bonds of benzene rings at 730 cm^{-1}, bands due to nonplanar vibrations (out-of-plane) of the C−H bonds at 748 and 782 cm^{-1}, and a band corresponding to the Ni−ligand vibrations mode at 915 cm^{-1} [59−61] (Table 4). The PP skeletal has been reported to cause bands in the ranges 772−777, 843−850, 999−1013, 1064−1078, 1360−1362, 1390−1392, and 1459−1483 cm^{-1}.[60] If the data reported for a determined phthalocyanine (or porphyrin) are compared for different metals in the organic ring, it is clear that the spectra are almost independent of the metal.[59−61] In Table 4 the reported data of some vibration normal modes for both skeletals (Figure 6) are compared with the calculated scaled spectra by quantum chemistry methods. The scale factor used for the frequencies was that defined by Scott and Radom for the method B3LYP/6-31G(d) (0.9802).[62] In general, we found that the calculated bands are in good agreement with the observed ones, although the calculated and the measured frequencies were obtained in the gas phase and in the solid phase (KBr pellets), respectively.

NiPc exhibits approximately D_{4h} symmetry, which predicts one IR-active M−N stretching,[59] but it is not improbable that due to the conjugated ring system more than one absorption peak appears, as occurs in Figure 6. This band, in spite of the strong bonding between the metal ion and the four surrounding nitrogen atoms in the pyrrolic rings, is dependent on the substituent in the peripheral rings and on the kind of ligand. Thus, for NiTAPc the Ni−N band is predicted from the theoretical calculations to 353 cm^{-1} and for NiTSPc is 362 cm^{-1}, both outside of the wavelength range used at experimental level. In the case of the PP complexes, the Ni−N band is predicted to be 272 cm^{-1} for both NiTAPP and NiTSPP. The lower frequencies obtained for the complexes with PP ligand can be understood in terms of the effect that the phenyl groups produces on the Ni−N normal mode limiting the vibrational motion in that region. In relation to the substituent groups, in NiTSPc the sulfonate group present frequencies for the asymmetric stretching at 1189 cm^{-1} and for the symmetric stretching at 1033 cm^{-1}. Similar values of 1184 cm^{-1} were measured for NiTSPP. The amino group appears near 3400 cm^{-1} in both amino complexes, 3328 cm^{-1} in NiTAPc, and 3440 cm^{-1} in NiTAPP. The comparison of these data with the theoretical results showed a very good agreement.

The calculated spectra of sulfonated complexes (NiTSPc, NiTSPP) predict a set of bands for the C−H stretching, as for the aromatic ring in the Pc ligand and the phenyl ring in the PP ligand, in the regions 3083−3099 cm^{-1} for Pc and 3076−3138 cm^{-1} for PP. As can be seen, these results are slightly shifted to lower energies with respect to the experimental value of 3436 cm^{-1} for both complexes. The C−C aromatic vibrational mode in NiTSPc, which is assigned experimentally to 1635 cm^{-1}, is predicted at the theoretical level in a wide range between 1543 and 1582 cm^{-1} for the vibration in the plane. In the case of NiTSPP, similar results are obtained, 1591−1625 cm^{-1} (in the plane).

The theoretical calculations for NiTSPc predict a range of values around 922 and 956 cm^{-1} for the S−O symmetric stretching of the experimental band at 1033 cm^{-1}. For the asymmetric stretching, we obtained values between 1172 and 1177 cm^{-1} for the corresponding experimental band at 1189 cm^{-1}. In the case of NiTSPP, the calculated symmetric bands associated with this vibrational mode appear between 933 and 942 cm^{-1}, very near to the experimental energy of 1040 cm^{-1}, and calculated asymmetric bands are between 1166 and 1180 cm^{-1}, also coinciding with the experimental energy of 1184 cm^{-1}. Under the observed band in 1033 (1040) cm^{-1} for NiTSPc (NiTSPP), we found a set of bands corresponding to the bending and torsion modes of the macrocycle skeletal, in agreement with the experimental results.

NiTAPc and NiTAPP complexes presented stretching NH bands of the amino groups at 3328 and 3440 cm^{-1}, respectively. The corresponding predicted bands are slightly shifted to higher frequencies, 3429−3090 cm^{-1} for NiTAPc and 3353−3641 cm^{-1} for NiTAPP. A good agreement was also found for the bending N−H with frequencies at 985 and 1172 cm^{-1} for NiTAPc and NiTAPP, respectively, which compares well with the predicted bands at 969 and 1139 cm^{-1}.

4. Conclusions

We have characterized by spectroscopic techniques (UV−vis, FTIR, and XPS) and quantum-chemical methods (B3LYP/LACVP(d)++) Ni(II)-substituted (sulfonate and amino) four porphyrin derivatives (NiTSPc, NiTAPc, NiTSPP, and NiTAPP). A comparison of the experimental and theoretical results indicates the following:

(1) In general, a good agreement has been found between the calculated and observed UV−vis bands. In the experimental spectra the more intense bands were the Q bands for the Pc ligand and the Soret band for the PP ligand. The theoretical analysis allowed us to assign in a rigorous way the electronic transitions occurring in each complex. We conclude that while the ligand effect is more important in the Q-band, the substituent effect is more significant in the Soret band.

(2) A good agreement was also found between the experimental and calculated infrared spectra. Using the theoretical results it was possible to assign bands to the experimental data. Unfortunately, it was not possible to compare the experimental with the calculated Ni−N band, since it was outside our experimental frequency range.

(3) NBO analysis giving the Lewis structure explains how the nickel atom interacts with the pyrrolic nitrogen atoms, a two-center bond between these atoms was not found. In contrast, and using second-order perturbation energy for all the complexes, a delocalization from one lone pair of each pyrrolic N toward one lone pair of the nickel atom is obtained.

(4) The Ni 2p XPS data unequivocally show that the change of the substituent ($-NH_2$ or $-SO_3$) in the porphyrin structure has little effect on the nature and characteristic binding energies of the Ni(II) present in these organometallic compounds.

Acknowledgment. We thank the financial support of the DICYT-USACh, FONDECYT Líneas Complementarias No. 8010006 and FONDECYT No. 1060203 projects from CONICYT-CHILE. C.B. thanks CONICYT for a doctoral fellowship.

References and Notes

(1) Ureta-Zañartu, M. S.; Berríos, C.; Pavez, J.; Zagal, J.; Gutiérrez, C.; Marco, J. F. *J. Electroanal. Chem.* **2003**, *553*, 147.
(2) Ureta-Zañartu, M. S.; Alarcón, A.; Berríos, C.; Cárdenas-Jirón, G. I.; Zagal, J.; Gutiérrez, C. *J. Electroanal. Chem.* **2005**, *580*, 94.
(3) Shen, Y.; Liu, J.; Jiang, J.; Liu, B.; Dong, S. *Electroanalysis* **2002**, *14*, 1557.
(4) Issahary, D. A.; Ginzburg, G.; Polak, M.; Meyerstein, D. *J. Chem. Soc., Chem. Commun*. **1982**, 441.
(5) Roslonek, G.; Taraszewska J. *J. Electroanal. Chem.* **1992**, *325*, 285.
(6) Trevin, S.; Beioui F.; Gómez-Villegas, M. G.; Bied-Charreton, C. *J. Mater. Chem.* **1997**, *7*, 923.
(7) Ozoemena, K. I.; Nyokong, T. *Talanta* **2005**, *67*, 162.
(8) Zhang, J.; Tse, Y.-H.; Pietro, W. J.; Lever, A. B. P. *J. Electroanal. Chem.* **1996**, *406*, 203.
(9) Cui, X.; Hong, L.; Lin X. *Anal. Sci.* **2002**, *18*, 543.
(10) Zhang, X.; Zhang, Y.; Jiang, J. *Spectrochim. Acta* **2004**, *60A*, 2195.
(11) Wael, K. D.; Westbroeck, P.; Bultnick, P.; Depla, D.; Vandenabeele, P.; Adriaens, A.; Temmerman, E. *Electrochem. Commun.* **2005**, *7*, 87.
(12) Liao, M.-S.; Warrs, J. D.; Huang, M.-J. *Inorg. Chem.* **2005**, *44*, 1941.
(13) Zhang, X.; Jiang, J. *J. Electron. Spectrosc. Relat. Phenom.* **2005**, *142*, 145.
(14) Karweik, D. H.; Winigrad, N. *Inorg. Chem.* **1976**, *15*, 2336.
(15) Sarno, D. M.; Matienzo, L. J.; Jones, W. E. J. *Inorg. Chem.* **2001**, *40*, 6308.
(16) Zagal, J. H.; Gulppi, M.; Isaacs, M.; Cárdenas-Jirón, G. I.; Aguirre, M. J. *Electrochim. Acta* **1998**, *44*, 1349.
(17) Zagal, J. H.; Gulppi, M. A.; Caro, C. A.; Cárdenas-Jirón, G. I. *Electrochem. Commun.* **1999**, *1*, 389.
(18) Zagal, J. H.; Gulppi, M. A.; Cárdenas-Jirón, G. I. *Polyhedron* **2000**, *19*, 2255.
(19) Zagal, J. H.; Cárdenas-Jirón, G. I. *J. Electroanal. Chem.* **2000**, *489*, 96.
(20) Cárdenas-Jirón, G. I.; Zagal, J. H. *J. Electroanal. Chem.* **2001**, *497*, 55.
(21) Cárdenas-Jirón, G. I.; Gulppi, M. A.; Caro, C. A.; del Río, R.; Páez, M.; Zagal, J. H. *Electrochim. Acta* **2001**, *46*, 3227.
(22) Cárdenas-Jirón, G. I. *J. Phys. Chem. A* **2002**, *106*, 3202.
(23) Cárdenas-Jirón, G. I. *Int. J. Quantum Chem.* **2003**, *91*, 389.
(24) Cárdenas-Jirón, G. I.; Parra-Villalobos, E. *J. Phys. Chem. A* **2003**, *107*, 11483.
(25) Caro, C. A.; Bedioui, F.; Páez, M.; Cárdenas-Jirón, G. I.; Zagal, J. H. *J. Electrochem. Soc.* **2004**, *151*, E32.
(26) Caro, C. A.; Zagal, J. H.; Bedioui, F.; Adamo, C.; Cárdenas-Jirón, G. I. *J. Phys. Chem. A* **2004**, *108*, 6045.
(27) Cárdenas-Jirón, G. I. *J. Chil. Chem. Soc.* **2004**, *49*, 101.
(28) Ríos-Escudero, A.; Costamagna, J.; Cárdenas-Jirón, G. I. *J. Phys. Chem. A* **2004**, *108*, 7253.
(29) Cárdenas-Jirón, G. I.; Espinoza-Leyton, F.; Sordo, T. L. *J. Chem. Sci.* **2005**, *117*, 515.
(30) Cárdenas-Jirón, G. I.; Caro, C. A.; Venegas-Yazigi, D.; Zagal, J. H. *J. Mol. Struct. (THEOCHEM)* **2002**, *580*, 193.
(31) Cárdenas-Jirón, G. I.; Venegas-Yazigi, D. *J. Phys. Chem. A* **2002**, *106*, 11938.
(32) Venegas-Yazigi, D.; Cárdenas-Jirón, G. I.; Zagal, J. H. *J. Coord. Chem.* **2003**, *56*, 1269.
(33) Paredes-García, V.; Cárdenas-Jirón, G. I.; Venegas-Yazigi, D.; Zagal, J. H.; Páez, M.; Costamagna, J. *J. Phys. Chem. A* **2005**, *109*, 1196.
(34) Cárdenas-Jirón, G. I.; Paredes-García, V.; Venegas-Yazigi, D.; Zagal, J. H.; Páez, M.; Costamagna, J. *J. Phys. Chem. A* **2006**, *110*, 11870.
(35) Cárdenas-Jirón, G. I.; Ríos-Escudero, A.; Costamagna, J.; Páez, M.; Zagal, J. H. Manuscript in preparation.
(36) Shirley, D. A. *Phys. Rev. B* **1972**, *5*, 4709.
(37) Wagner, C. D.; Davis, L. E.; Zeller, M. V.; Taylor, J.; Raymond, R. M.; Gall, L. H. *Surf. Interface Anal.* **1981**, *3*, 211.
(38) (a) Lee, C.; Yang, W.; Parr, R. G. *Phys. Rev.* B **1988**, *37*, 785. (b) Miehlich, B.; Savin, A.; Stoll, H.; Preuss, H. *Chem. Phys. Lett.* **1989**, *157*, 200. (c) Becke, A. D. *J. Chem. Phys.* **1993**, *98*, 5648.
(39) *Jaguar 6.5*; Schrodinger, LLC: Portland, OR, 1991−2005.
(40) Glendening, E. D.; Badenhoop, J. K.; Reed, A. E.; Carpenter, J. E.; Bohmann, J. A.; Morales, C. M.; Weinhold, F. *NBO 5.0*; Theoretical Chemistry Institute, University of Wisconsin: Madison, WI, 2001; http://www.chem.wisc.edu/~nbo5.
(41) Scudiero, L.; Barlow, Dan, E.; Hipps, K. W. *J. Phys. Chem. B* **2000**, *104*, 11899.
(42) Ghosh, A.; Fitzgerald, J.; Gassman, P. G.; Almlöf, J. *Inorg. Chem.* **1994**, *33*, 6057.
(43) Sarno, D. M.; Matienzo, L. J.; Jones, W. E., Jr. *Inorg. Chem.* **2001**, *40*, 6308.
(44) Karweik, D. H.; Winograd, N. *Inorg. Chem.* **1976**, *15*, 2336.
(45) Ghosh, A. *J. Org. Chem.* **1993**, *58*, 6932.
(46) Gassman, P.; Ghosh, A.; Almlöf, J. *J. Am. Chem. Soc.* **1992**, *114*, 990.
(47) Alfredsson, Y.; Brena, B.; Nilson, K.; Ahlund, J.; Kjeldgaard, L.; Nyberg, M.; Luo, Y.; Martensson, N.; Sandell, A.; Puglia, C.; Siegbahn, H. *J. Chem. Phys.* **2005**, *122*, 214723.
(48) Malinski, T.; Ciszewlski, A.; Bennet, J.; Fish, J. R. *J. Electrochem. Soc.* **1991**, *138*, 2008.
(49) Muralidharan, S.; Hayes, R. G. *J. Phys. Chem.* **1979**, *71*, 2970.
(50) Ottaviano, L.; de Mardo, S.; Lozzi, L.; Passacantando, M.; Picozzi, P.; Santucci, S. *Surf. Sci.* **1997**, *373*, 318.
(51) Tackley, D. R.; Dent, G.; Smith, W. E. *Phys. Chem. Chem. Phys.* **2001**, *3*, 1419.
(52) Liao, M.-S.; Scheiner, S. *J. Chem. Phys.* **2001**, *114*, 9780.
(53) Parr, R.; Yang, W. *J. Am. Chem. Soc.* **1983**, *105*, 7512.
(54) Pan, Y.; Chen, W.; Lu, S.; Zhang, Y. *Dyes Pigm.* **2005**, *66*, 115.
(55) Gouterman, M. In *The Porphyrins*, *Vol. III, Part A, Physical Chemistry*; Dolphin, D., Ed.; Academic Press: New York, 1978.
(56) Gouterman, M. *J. Mol. Spectrosc.* **1961**, *6*, 138.
(57) Gouterman, M.; Wagnière, G. H.; Snyder, L. C. *J. Mol. Spectrosc.* **1963**, *11*, 108.
(58) Nakamoto, K. *Infrared and Raman Spectra of Inorganic and Coordination Compounds*, 4th ed.; J. Wiley & Sons: New York, 1986; p 63.
(59) El-Nahass, M. M.; Abd-El-Rahman, K. F.; Darwish, A. A. A. *Mater. Chem. Phys.* **2005**, *92*, 185.
(60) El-Nahass, M. M.; Farag, A. M.; Abd El-Rahman, K. F.; Darwish, A. A. A. *Opt. Laser Technol.* **2005**, *37*, 513.
(61) Achar, B. N.; Lokesh, K. S. *J. Organomet. Chem.* **2004**, *689*, 3357.
(62) Scott, A. P.; Radom, L. *J. Phys. Chem.* **1996**, *100*, 16502.